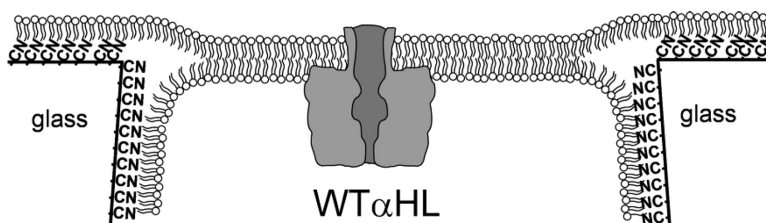Article

Single Ion-Channel Recordings Using Glass Nanopore Membranes

Ryan J. White, Eric N. Ervin, Tinglu Yang, Xin Chen, Susan Daniel, Paul S. Cremer, and Henry S. White

More About This Article

Additional resources and features associated with this article are available within the HTML version:

- Supporting Information
- Links to the 7 articles that cite this article, as of the time of this article download
- Access to high resolution figures
- Links to articles and content related to this article
- Copyright permission to reproduce figures and/or text from this article

View the Full Text HTML

J|A|C|S

A R T I C L E S

Single Ion-Channel Recordings Using Glass Nanopore Membranes

Ryan J. White,[†] Eric N. Ervin,[†] Tinglu Yang,[‡] Xin Chen,[‡] Susan Daniel,[‡]
Paul S. Cremer,*,[‡] and Henry S. White*,[†]

Contribution from the Department of Chemistry, University of Utah, 315 S 1400 E, Salt Lake City, Utah 84112, and Department of Chemistry, Texas A&M University, P.O. Box 30012, College Station, Texas 77842-3012

Received May 4, 2007; E-mail: cremer@mail.chem.tamu.edu; white@chem.utah.edu

Abstract: Protein ion-channel recordings using a glass nanopore (GNP) membrane as the support structure for lipid bilayer membranes are presented. The GNP membrane is composed of a single conical-shaped nanopore embedded in a ~50 μm-thick glass membrane chemically modified with a 3-cyanopropyldimethylchlorosilane monolayer to produce a surface of intermediate hydrophobicity. This surface modification results in lipid monolayer formation on the glass surface and a lipid bilayer suspended across the small orifice (100−400 nm-radius) of the GNP membrane, while allowing aqueous solutions to fully wet the glass nanopore. The GNP membrane/bilayer structures, which exhibit ohmic seal resistances of ~70 GΩ and electrical breakdown voltages of ~0.8 V, are exceptionally stable to mechanical disturbances and have lifetimes of at least 2 weeks. These favorable characteristics result from the very small area of bilayer (10^{-10}–10^{-8} cm^2) that is suspended across the GNP membrane orifice. Fluorescence microscopy and vibrational sum frequency spectroscopy demonstrate that a lipid monolayer forms on the 3-cyanopropyl-dimethylchlorosilane modified glass surface with the lipid tails oriented toward the glass. The GNP membrane/bilayer structure is well suited for single ion-channel recordings. Reproducible insertion of the protein ion channel, wild-type α-hemolysin (WTαHL), and stochastic detection of a small molecule, heptakis-(6-O-sulfo)-β-cyclodextrin, are demonstrated. In addition, the insertion and removal of WTαHL channels are reproducibly controlled by applying small pressures (−100 to 350 mmHg) across the lipid bilayer. The electrical and mechanical stability of the bilayer, the ease of which bilayer formation is achieved, and the ability to control ion-channel insertion, coupled with the small bilayer capacitance of the GNP membrane-based system, provide a new and nearly optimal system for single ion-channel recordings.

Introduction

For over three decades, the insertion of transmembrane protein channels into supported lipid bilayers for ion-channel measurements has been an integral tool for investigating the biophysical properties of protein channels[1−4] as well as for quantifying the interactions of protein channels with receptor molecules.[5−10] Recently, application of protein ion channels supported in lipid bilayers has been proposed for designing biosensors[11] and the sequencing of DNA.[12−15] Single ion-channel recordings are traditionally performed using planar lipid bilayers supported across 30 to 100 μm-diameter orifices in Teflon, Delrin, polysulfone, or other suitable hydrophobic polymer-based membranes.[16] This well-established technique possesses several disadvantages that are associated with the large orifice dimensions, severely limiting the development of high-throughput and robust ion-channel recording systems. In particular, the lipid bilayer supported on a large diameter orifice is sensitive to pressure fluctuations, mechanical vibrations, and electrical disturbances and is thus highly susceptible to failure (rupture) within hours or even minutes after formation. In addition, Wonderlin and co-workers also note that the lipid bilayer capacitance is a major contributor to overall system noise in ion-channel recordings.[17] A reduction of bilayer capacitance

[†] University of Utah.
[‡] Texas A&M University.
(1) Mayer, M.; Kriebel, J. K.; Tosteson, M. T.; Whitesides, G. M. *Biophys. J.* **2003**, *85*, 2684−2695.
(2) Cannon, B.; Hermansson, M.; Györke, S.; Somerharju, P.; Virtanen, J. A.; Cheng, K. H. *Biophys. J.* **2003**, *85*, 933−942.
(3) Jung, Y.; Cheley, S.; Braha, O.; Bayley, H. *Biochemistry* **2005**, *44*, 8919−8929.
(4) Miles, G.; Cheley, S.; Braha, O.; Bayley, H. *Biochemistry* **2001**, *40*, 8514−8522.
(5) Gu, L.; Braha, O.; Conlan, S.; Cheley, S.; Bayley, H. *Nature* **1999**, *398*, 686−690.
(6) Gu, L.; Bayley, H. *Biophys. J.* **2000**, *79*, 1967−1975.
(7) Bayley, H.; Braha, O.; Gu, L. *Adv. Mater.* **2000**, *12*, 139−142.
(8) Rostovtseva, T. K.; Nestorovich, E. M.; Bezrukov, S. M. *Biophys. J.* **2002**, *82*, 160−169.
(9) Hirano, A.; Wakabayashi, M.; Matsuno, Y.; Sugawara, M. *Biosens. Bioelectron.* **2003**, *18*, 973−983.
(10) Shin, S.; Bayley, H. *J. Am. Chem. Soc.* **2005**, *127*, 10462−10463.
(11) Bayley, H.; Cremer, P. S. *Nature* **2001**, *413*, 226−230.
(12) Kasianowicz, J. J.; Brandin, E.; Branton, D.; Deamer, D. W. *Proc. Natl. Acad. Sci. U.S.A.* **1996**, *93*, 13770−13773.
(13) Howorka, S.; Cheley, S.; Bayley, H. *Nat. Biotechnol.* **2001**, *19*, 636−639.
(14) Akeson, M.; Branton, D.; Kasianowicz, J. J.; Brandin, E.; Deamer, D. W. *Biophys. J.* **1999**, *77*, 3227−3233.
(15) Nakane, J.; Wiggin, M.; Marziali, A. *Biophys. J.* **2004**, *87*, 615−621.
(16) Montal, M.; Mueller, P. *Proc. Nat. Acad. Sci. U.S.A.* **1972**, *69*, 3561−3566.
(17) Wonderlin, W. F.; Finkel, A.; French, R. J. *Biophys. J.* **1990**, *58*, 289−297.

using smaller diameter orifices potentially allows for increased current and temporal resolution in ion-channel recordings.[17] Mayer et al. reported ion-channel recordings using supported lipid bilayers on orifices as small as 2 μm in diameter across an amorphous Teflon membrane.[1] To the best of our knowledge, this is the smallest *single* orifice that has been reported to date for ion-channel recordings.

Significant improvements in lipid bilayer stability for ion-channel measurements have been achieved by sandwiching the bilayer between viscous polymeric and gel-phase materials.[18,19] Most recently, Gu and co-workers[20] introduced a portable and durable bilayer chip platform for single ion-channel measurements in which a lipid bilayer spanning a 100 μm-diameter aperture is sandwiched between two agarose gel layers. These investigators reported a high success rate in transporting a bilayer containing a single transmembrane protein, a bilayer breakdown voltage of ~325 mV, and a durability of 65 h with continuous bilayer and stochastic detection using a protein sensing unit. Bayley and co-workers reported a very similar system that, in addition, allows for continuous storage of a bilayer containing a single transmembrane protein for up to 3 weeks at 4 °C and the capability of withstanding rigorous mechanical disruptions.[21] It should be noted, however, that the temporal sampling responses of these ion-channel systems are limited because of the need for the analyte to diffuse across the gel layers. For instance, Gu and co-workers obtained a steady-state response in 40 min using 1000 μm-thick agarose layers. Other attempts at improving bilayer stability have employed the use of tethered lipid bilayers[22] and polymerizable lipid bilayers.[23]

Herein, we report a glass nanopore (GNP) membrane support for ion-channel recordings that allows for the formation of exceptionally stable bilayers with orifice areas that are a million-fold smaller than those recently reported by Gu, Bayley, and co-workers.[20,21] The GNP membrane, schematically shown in Figure 1A, is a single conical nanopore embedded in a thin glass membrane (~50 μm), with an orifice radius as small as 10 nm. The GNP is fabricated using simple benchtop methods recently described by this laboratory.[24] Because of favorable interactions of the polar head groups of the lipid molecules and the hydrophilic glass surface, a lipid bilayer can be readily deposited at the outer surface of the unmodified GNP membrane to yield a *supported* bilayer across the pore orifice, as previously reported by our laboratories.[25] Fertig et al. also reported the application of unmodified planar glass chips for ion-channel recordings, in which a small aperture in the glass chip (1−50 μm) was formed by ion-track etching.[26−28] The supported bilayer configuration,
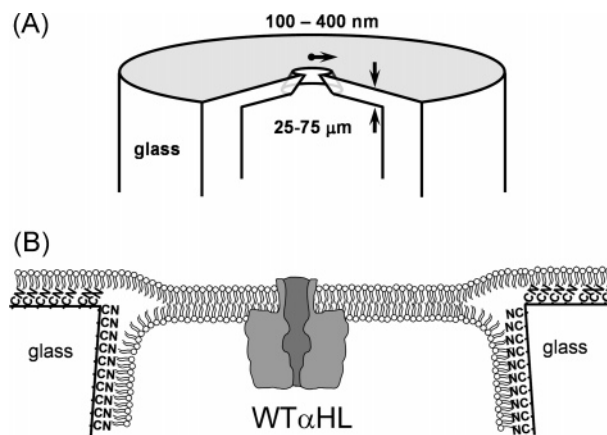

Figure 1. (A) Schematic drawing of the GNP membrane (not drawn to scale); (B) schematic illustration of the spanning bilayer structure at the orifice of the GNP membrane. Modification of the glass nanopore surface with 3-cyanopropyldimethylchlorosilane causes the hydrophobic tail group of the lipid to orient toward the surface. The bilayer forms only over the pore opening and corrals the transmembrane protein at the GNP orifice.

however, is not ideally suited for ion-channel recordings because of the leakage of current through the thin water layer (~1 nm thick) that exists between the polar head groups of the lipids and the glass surface.[25] Herein, we report methods that allow for formation of a *suspended* lipid bilayer, depicted in Figure 1B, in which lipid monolayers deposited on both the interior and exterior surfaces of the GNP merge to form exceptionally stable bilayers across the GNP orifice. To successfully fabricate this structure for a working ion-channel recording device, we hypothesized that the interior and exterior surfaces could be chemically modified to produce a glass surface that is sufficiently hydrophobic to allow deposition of a monolayer of lipid molecules with the hydrophobic tails oriented toward the glass surface, while at the same time maintaining sufficient hydrophilic surface character allowing an aqueous solution to fill the nanopore. We have discovered that deposition of 3-cyanopropyldimethylchlorosilane on the GNP surface, which creates a silane monolayer with a terminal −CN functionality, allows for both the formation of the *suspended* bilayer structure shown in Figure 1B and the wetting of the nanopore by aqueous solutions. In addition, the −CN functionality prevents protein adsorption on glass, as initially reported by Wayment and Harris.[29]

The GNP membrane/bilayer structure shown in Figure 1B and described later exhibits typical seal resistances of ~70 GΩ and can be formed over pore orifices ranging from tens of nanometers to several micrometers on glass and quartz. Protein ion-channel recordings have been performed with GNP orifice radii as small as 100 nm (vide infra). The application of a 100 nm-radius orifice results in a 10^6-fold reduction in the bilayer area in comparison to conventional ion-channel measurements and exhibits greatly improved mechanical and electrical stability. The GNP membrane platform has successfully been used in single ion-channel recordings employing the transmembrane protein, wild-type α-hemolysin (WTαHL) from *Staphylococcus aureas*, and the subsequent stochastic sensing of the small molecule, heptakis(6-O-sulfo)-β-cyclodextrin (s$_7\beta$CD). The GNP membrane/bilayer structure exhibits a voltage stability of ~800

(18) Beddow, J. A.; Peterson, I. R.; Heptinstall, J.; Walton, D. J. *Anal. Chem.* **2004**, *76*, 2261−2265.
(19) Jeon, T.; Malmstadt, N.; Schmidt, J. J. *J. Am. Chem. Soc.* **2005**, *128,* 42−43.
(20) Shim, J. W.; Gu, L. Q. *Anal. Chem.* **2007**, *79*, 2207−2213.
(21) Kang, X.; Cheley, S.; Rice-Ficht, A. C.; Bayley, H. *J. Am. Chem. Soc.* **2007**, *129*, 4701−4705.
(22) Cornell, B. A.; Braach-Maksvytis, V. L. B.; King, L. G.; Osman, P. D. J.; Raguse, B.; Wieczorek, L.; Pace, R. J. *Nature* **1997**, *387*, 580−583.
(23) Shenoy, D. K.; Barger, W. R.; Singh, A.; Panchal, R. G.; Misakian, M.; Stanford, V. M.; Kasianowicz, J. J. *Nano Lett.* **2005**, *5*, 1181−1185.
(24) Zhang, B.; Galusha, J.; Shiozawa, P. G.; Wang, G.; Bergren, A. J.; Jones, R. M.; White, R. J.; Ervin, E. N.; Cauley, C.; White, H. S. *Anal. Chem.* **2007**, *79*, 4778−4787.
(25) White, R. J.; Zhang, B.; Daniel, S.; Tang, J. M.; Ervin, E. N.; Cremer, P. S.; White, H. S. *Langmuir* **2006**, *22*, 10777−10783.
(26) Fertig, N.; Blick, R. H.; Behrends, J. C., *Biophys. J.* **2002**, *82*, 3056−3062.
(27) Fertig, N.; Klau, M.; George, M.; Blick, R. H.; Behrends J. C. *App. Phys. Lett.* **2002**, *81*, 4865−4867.
(28) Fertig, N.; Meyer, C.; Blick, R. H.; Trautmann, C.; Behrends, J. C.; *Phys. Rev. E* **2004**, *64* 040901-1−04091-4.
(29) Wayment, J. R.; Harris, J. M. *Anal. Chem.* **2006**, *78*, 7841−7849.

mV, greatly surpassing the value of 325 mV recently reported by Gu and co-workers[20] and a reported value of 460 mV for Teflon pores with diameters less than 40 μm.[1] Although extensive stability studies have not yet been performed, the GNP membrane/bilayer lifetime is at least 2 weeks at room temperature, and continuous stochastic detection with a WTαHL sensor unit has been achieved for at least 24 h without further optimization. The GNP membrane/bilayer structure is stable to mechanical disruptions and can be transferred between different analyte solutions with a functioning WTαHL sensing unit remaining in place. In addition to these highly favorable properties, we have discovered the ability to control the insertion and removal of single ion channels from the bilayer by applying small pressure gradients across lipid bilayers suspended over the GNP orifice. This intriguing discovery allows ion channels to be sequentially, and repeatedly, inserted and removed from the same bilayer, an ability that may prove to be a critical process component for directed insertion of proteins at different positions on an array of ion-channel biosensors.[11]

Experimental Section

Chemicals. KCl, K$_2$HPO$_4$, and KH$_2$PO$_4$ (Mallinckrodt) were used as received. All aqueous solutions were prepared using water (>18 MΩ·cm) from a Barnstead E-pure water purification system. A buffered electrolyte of 1.0 M KCl and 10 mM potassium phosphate buffer (PBS solution) at a pH of 7.4 was made by dissolving appropriate amounts of each salt in ultrapure water. All references herein to PBS buffer solution refer to this solution composition. The phospholipids, 1,2-dimyristoyl-*sn*-glycero-3-phosphocholine (DMPC), 1-palmitoyl-2-oleoyl-*sn*-glycero-3-phosphocholine (POPC), and 1,2-diphytanoyl-*sn*-glycero-3-phosphocholine (DPhPC) were purchased from Avanti Polar Lipids (Alabaster, AL). *N*-(Texas Red sulfonyl)-1,2-dihexadecanoyl-*sn*-glycero-3-phosphoethanolamine (Texas Red DHPE) was purchased from Molecular Probes (Eugene, OR). Acetonitrile (HPLC grade, J. T. Baker) was stored over 3-Å molecular sieves. 3-Cyanopropyldimethylchlorosilane (Cl(Me)$_2$Si(CH$_2$)$_3$CN) (Gelest Inc.) was used as received. Wild-type α-hemolysin, WTαHL (lyophilized powder, monomer, Sigma-Aldrich), was dissolved into 1.0 M KCl 10 mM PBS buffer solution (pH 7.4) and stored at −80 °C when not in use. Heptakis(6-*O*-sulfo)-β-cyclodextrin (s$_7\beta$CD) (Fluka) was used as received.

Glass Nanopore (GNP) Membranes. A benchtop method for fabricating GNP membranes was first reported in ref 25 and recently described in detail in ref 24. Briefly, the sharpened end of an electrochemically etched 25 μm-diameter Pt wire (with half-cone angle, θ, of 10 ± 1°) is sealed to a depth of between 25 and 75 μm into one end of a soda-lime glass capillary that is heated to softening using a H$_2$/air flame[24] (Dagan Corporation SB16 capillaries, 1.65-mm o.d., 0.75-mm i.d.; softening point 700 °C; manufacturer provided composition: 67.7% SiO2, 2.8% BaO, 15.6% Na2O, 5.6% CaO, 4% MgO, 1.5% B, and 0.6% K$_2$O%).[24] After cooling, the glass capillary is polished to expose a Pt nanodisk electrode shrouded in glass. The polishing step is performed while monitoring the electrical conductivity between the Pt wire and the wetted polishing surface to determine and control the size of the exposed disk.[24] The Pt disk is then briefly electrochemically etched, after which the entire Pt wire is gently pulled from the glass to yield a conical-shaped nanopore. Full details of the fabrication process are presented in ref 24. A photograph of the GNP membrane platform is shown in Figure 2A. The radius of the small opening of the GNP (r_i) is computed from the dc electrical ohmic resistance (R) of the GNP measured in a 1.0 M KCl solution at room temperature, using the expression $r_i = 19/R$.[25] The relative uncertainty in r_i is estimated be ~10%.[25]

Glass Silanization. GNP membranes are pretreated before silanization by soaking the entire glass capillary (inside and outside) in a 0.1
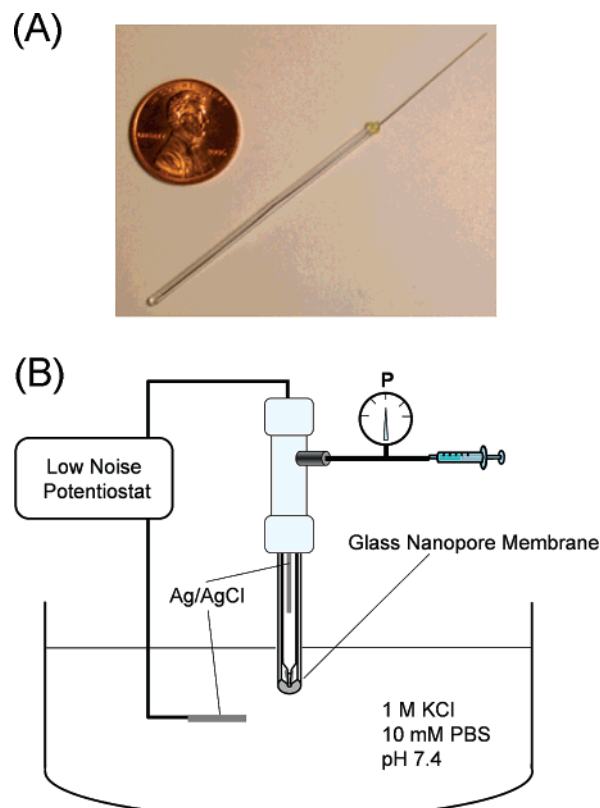
Figure 2. (A) Photograph of a GNP membrane at the end of a glass capillary (3 cm length; i.d. = 0.75; o.d. = 1.65 mm). A Ag/AgCl electrode is inserted into the capillary for ion-channel measurements. (B) Schematic of the experimental setup (see text for details).

M HNO$_3$ solution for 10 min. The glass capillary is rinsed with copious amounts of ultrapure H$_2$O followed by CH$_3$CN. The GNP membranes are then filled and fully immersed in a 2% v/v solution of 3-cyanopropyldimethlychlorosilane in CH$_3$CN for 12 h to ensure surface modification of both the internal and external surfaces. The capillary is rinsed sequentially with CH$_3$CN, EtOH, and H$_2$O followed by air drying. Modified GNP membranes can be stored dry indefinitely for later use in ion-channel recordings.

Electrical Measurements. All electrical measurements were performed with a Dagan Chem-Clamp Low Noise potentiostat interfaced to a PC via in-house written LabVIEW (National Instruments) programs. Current−voltage (i−V) and current−time (i−t) recordings were performed by applying a voltage between two Ag/AgCl electrodes positioned inside and outside of the GNP capillary. The Ag/AgCl electrodes were prepared by oxidation of clean Ag wires (0.5 mm-diameter) in a saturated FeCl$_3$ solution for ~60 s. A schematic illustration of the experimental setup is presented in Figure 2B. The voltages reported herein are referenced to the Ag/AgCl electrode positioned inside of the capillary.

Bilayer Formation. Bilayer formation was accomplished using a painting method as described by Alvarez.[39] Herein, "priming" refers to the process of bringing a plastic pipet tip containing the lipid solution to the GNP membrane surface and the deposition of the solution onto this surface. "Painting" refers to lightly moving a clean pipet tip (no lipid solution) across the primed GNP membrane surface to form a lipid bilayer over the nanopore orifice.

Following silanization, the outer surface near the pore is primed with ~10 μL of a 10 mg/mL solution of a lipid dissolved in decane. Lipids used in the ion-channel recording experiments were either POPC or DPhPC. Excess solvent is evaporated using a stream of N$_2$, and the capillary is filled with the PBS buffer solution (pH 7.4) or the same solution containing a transmembrane protein. With the end of the GNP

membrane fully immersed in the PBS buffer solution (pH 7.4), the outer surface is re-primed with ~10 μL of the lipid/decane solution. A clean plastic pipet tip is then lightly dragged across the exterior GNP membrane surface to paint a lipid bilayer over the nanopore. The ionic current through the GNP is continuously monitored during the painting procedure to determine successful bilayer formation. The sudden increase in pore resistance from ~10^6 to ~10^{11} Ω is typical of successful bilayer formation across the orifice, as subsequently demonstrated by the measurement of ion-channel conductance values that agree with literature values.

Properly formed bilayers on the GNP membrane that are used in ion-channel recordings have a breakdown voltage of ~0.78 V (vide infra). Thus, the existence of a bilayer, prior to protein insertion, was checked by application of a $\pm$ 1 V bias across the bilayer, consistent with techniques used in conventional planar bilayer measurements. Following electrical breakdown, the bilayer was repainted and employed in ion-channel recordings. In the event that there was no voltage-induced breakdown, the nanopore was presumed clogged with the lipid solution. The nanopore orifice could be unclogged by repeatedly dragging a clean pipet tip across the surface while applying $\pm$1 V until the conductance returned to the open nanopore value. A bilayer can then often be formed on the previously clogged GNP orifice by painting with a clean pipet tip.

Transmembrane Pressure Control. As detailed below, a positive pressure across the membrane is required to insert transmembrane proteins into a bilayer suspended across the GNP orifice. The pressure across the bilayer membrane was controlled by inserting the open end of the GNP into a pipet holder (DAGAN) that was connected to a 10 mL gastight syringe (Hamilton), as shown in Figure 2B. The pressure was monitored continuously using a sphygmomanometer (pressure sensing range of −100 to 300 mmHg) as shown in Figure 2B. All transmembrane pressures reported herein are referenced to the exterior (ambient) solution pressure. A small positive pressure inside the capillary could also be obtained by simply sealing the end of the capillary with a small plug of silicon rubber, allowing the Ag/AgCl wire to protrude through the silicon rubber. This sealing compresses the air and aqueous solution inside the capillary, creating a positive transmembrane pressure.

Lipid Bilayer and Monolayer Preparation for Lipid Film Structural Analysis. Small unilamellar vesicles (SUV) were fused to glass substrates by vesicle fusion.[30−32] Vesicles comprising POPC lipids doped with 0.1 mol % Texas Red DHPE lipids were used for the fluorescence microscopy experiments. DMPC vesicles were used for vibrational sum frequency spectroscopy (VSFS) experiments. The appropriate composition of lipids were dissolved and mixed in chloroform and then dehydrated under vacuum for 3 h. The dried mixture was rehydrated in the PBS buffer solution (pH 7.4) and subjected to ten freeze/thaw cycles by alternating between liquid nitrogen and a 30 °C water bath. The solution was then extruded several times through a polycarbonate filter to produce vesicles of uniform size. The solution was extruded first through a filter with 100 nm diameter pores, followed by five passes through a filter with 50 nm diameter pores. The resultant SUVs were found to have an average diameter of 80−90 nm as determined by light scattering using a 90Plus Particle Size Analyzer (Brookhaven Instruments Corporation).

The glass coverslips used as supports for the bilayers were cleaned in 7X solution (MP Biomedicals, Aurora, OH) following established procedure.[33] The coverslips were then annealed in an oven at 500 °C for 5 h to yield flat surfaces with a typical root-mean-square (rms)

roughness value of 0.13 nm over a 1 μm^2 area as determined by atomic force microscopy (AFM). Glass slides were then modified with 3-cyanopropyldimethylchlorosilane in the same manner as described above for GNP modification. A 100 μL drop of vesicle solution was placed on silanized glass coverslips as well as on unmodified (bare) glass coverslips which were employed as a control. The solution was confined to a circular area in the center of the glass by a thin hydrophobic PDMS mold. The mold was made by crosslinking PDMS between two silanized glass microscope slides separated by a thin metal spacer between 200 and 400 μm thick. After crosslinking, a circular hole ~1 cm in diameter was punctured through the elastomeric sheet using a hole punch. The outer edges of the mold were trimmed to fit exactly over the glass coverslip without hanging off.

The vesicle solution was incubated on the glass slides for 10 min and rinsed with copious amounts of buffer to remove any excess, unfused vesicles from the surface. Following the rinse, surfaces where gently scratched by a pair of metal tweezers to remove lipid from a small portion of the substrate to create a zero fluorescence baseline. These samples were subsequently rinsed before imaging under an inverted epifluorescence Nikon Eclipse TE 2000-U microscope equipped with a Sensys CCD camera (Photometrics, Roper Scientific).

Mobility Measurements. Diffusion coefficients and mobile fractions of the lipids were measured by fluorescence recovery after photo-bleaching (FRAP).[34] A circular patch of the bilayer containing fluorescently labeled lipids was bleached with the 568.2 nm line from a mixed gas Ar$^+$/Kr$^+$ laser beam (Stabilite 2018, Spectra Physics). A beam of 100 mW of power was directed onto the sample for less than 1 s. The beam, which was sent through a 10X objective, had a full-width at half-maximum of ~17 μm at the sample plane. The recovery of the photobleached spot was followed as a function of time using time-lapse imaging under a fluorescence microscope (Nikon Eclipse TE2000-U) equipped with a Sensys CCD camera (Photomatrics, Roper Scientific) working in conjunction with MetaMorph software (Universal Imaging). The fluorescence intensity of the bleached spot was determined after background subtraction and normalization for each image. The diffusion coefficient of the lipids was determined using standard procedures.[34] Briefly a single-exponential equation was used fit to the fluorescence recovery as a function of time, from which the mobile fraction of the lipids and the half-time of recovery ($t_{1/2}$) could be obtained. The diffusion coefficient, D, was then calculated using the following equation:[34]

$$D = \frac{w^2}{4t_{1/2}}\gamma \tag{1}$$

where w is the full width at half-maximum of the Gaussian profile of the focused beam and γ is a correction factor that depends on the bleach time and geometry of the laser beam. In these experiments $w = 17$ μm and $\gamma = 1.1$.

Vibrational Sum-Frequency Spectroscopy. VSFS measurements were performed with a passive−active mode-locked Nd:YAG laser (PY61c, Continuum, Santa Clara, CA) equipped with a negative feedback loop in the oscillator cavity to provide enhanced shot-to-shot stability. The 1064 nm beam has a pulse width of 21 ps and operates at a repetition rate of 20 Hz. It is used to pump an optical parametric oscillator (OPA) stage (Laser Vision, Bellevue, WA) that generates the 532 nm and tunable infrared input beams (2800−4000 cm^{-1}). The IR and visible beams are overlapped at the sample interface with incident angles of 51° and 42°, respectively, with respect to the surface normal. All sum frequency spectra are taken with the SSP polarization combination, referring to the sum frequency, visible and infrared beams, respectively. Each data set is normalized to spectra taken from a piece of Y-cut crystalline quartz.

(30) Brian, A. A.; McConnell, H. M. *Proc. Natl. Acad. Sci.* **1984**, *81*, 6159−6163.
(31) Groves, J. T.; Ulman, N.; Cremer, P. S.; Boxer, S. G. *Langmuir* **1998**, *14*, 3347−3350.
(32) Cremer, P. S.; Groves, J. T.; Kung, L. A.; Boxer, S. G. *Langmuir* **1999**, *15*, 3893−3896.
(33) Yang, T. L.; Jung, S. Y.; Mao, H. B.; Cremer, P. S. *Anal. Chem.* **2001**, *73*, 165−169.

(34) Axelrod, D.; Koppel, D. E.; Schlessinger, J.; Elson, E.; Webb, W. W. *Biophys. J.* **1976**, *16*, 1055−1069.

Results and Discussion

Silanization of GNP Membrane and Suspended Bilayers.
The suspended lipid bilayer structure depicted in Figure 1B is a consequence of the deposition of lipids on the interior and exterior surfaces of the chemically modified GNP membrane with the hydrophobic tails oriented toward the glass surface. As discussed in the Introduction, the key criterion for formation of a suspended bilayer for ion-channel recordings is that the glass surface is modified to impart sufficient hydrophobic character allowing the lipid tails-down configuration, while still maintaining a sufficiently hydrophilic character allowing aqueous solutions to wet the nanopore. Wetting is often cited as a common problem when working with pores of nanoscale dimensions.[35]

After fabrication and characterization of the GNP membrane, as described in the Experimental Section, the glass surface is silanized with 3-cyanopropyldimethylchlorosilane. Because this silane contains a single reactive Si−Cl bond, the surface chemical modification yields a monolayer that exposes a terminal−CN group to the solution, as previously discussed in relation to modification of functionalized GNP electrodes.[36] The water contact angle (θ_c) of the modified glass surface is 55°, which falls between angles that classify surfaces as either strongly hydrophilic or hydrophobic.[37] Spectroscopic measurements and fluorescence microscopy presented below explore how chemical modification using 3-cyanopropyldimethylchlorosilane controls the structure, function, and orientation of lipid layers at the modified glass/water interface.

Following the deposition of the -CN terminated silane monolayer on the interior and exterior surfaces of the GNP membrane, a lipid/decane (10 mg lipid/1 mL decane) solution is painted across the exterior surface (Experimental Section)[38,39] resulting in the formation of a lipid monolayer on the glass surfaces and a lipid bilayer that is suspended across the GNP orifice. Both POPC and DPhPC were used for this purpose with similar results. We have found that painting the lipid/decane solution reproducibly yields GNP membrane/bilayer seal resistances between 30 and >100 GΩ, with an average value of ∼71 ± 30 GΩ based on ∼20 independent measurements. For instance, Figure 3 shows $i−V$ curves comparing the behavior of a 150 nm-radius silanized GNP membrane prior to and following the painting of a DPhPC/decane solution across the orifice. In these measurements, the GNP capillary is filled with the PBS buffer solution (pH 7.4) and placed in a 10 mL solution of the same composition. The ionic current is measured as a function of the voltage scanned at 20 mV/s between internal and external Ag/AgCl electrodes. As determined from the slopes of the $i−V$ curves, the silane modified GNP membrane has an open pore resistance of 1.3 MΩ (labeled "Open GNP"). The same GNP membrane after lipid painting and bilayer formation exhibits a seal resistance of 88 GΩ (labeled "GNP/Bilayer"). The fact that a lipid bilayer is indeed suspended across the GNP
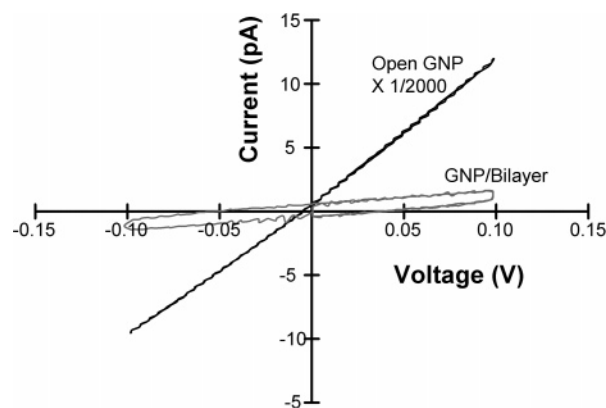

Figure 3. $i−V$ curves for a 150 nm-radius GNP in 1.0 M KCl 10 mM PBS buffer at pH 7.4. The open-pore $i−V$ curve is scaled by 1/2000 (labeled "Open GNP") for comparison to the same structure after DPhPC bilayer deposition across the orifice (labeled "GNP/Bilayer"). The open-pore and bilayer-seal resistance are 1.3 MΩ and 88 GΩ, respectively.

orifice will be demonstrated by the ion-channel recordings presented below. We have found that lipid bilayers are readily deposited on GNP membranes with orifices as small as 100 nm and as large as 4 μm, as well on nanopore membranes prepared from quartz instead of soda-lime glass. The lipid bilayer can be removed by briefly (∼1 s) subjecting the bilayer to a transmembrane potential of >1 V and can be redeposited on the silanized GNP by painting as described above. Conversely, the lipid layers may also be removed by immersing the GNP capillary in ethanol, and then (after rinsing the capillary with H$_2$O), reformed by painting. Silanized GNP membranes are reusable for lipid deposition and ion-channel recordings over several months without the need for additional resilanization.

Characterization of Lipid Monolayers on Chemically Modified Glass Surfaces. We present experiments demonstrating that lipid molecules form a uniform monolayer on cyano-terminated silanized glass substrates in a tails-down configuration. To demonstrate this, we first compared the fluorescence level of a POPC film fused to a hydrophilic bare glass substrate and a cyano-terminated substrate. Each bilayer was doped with 0.1 mol % Texas Red DHPE for visualization purposes. Glass substrates were cleaned following standard procedures, yielding uniformly hydrophilic surfaces.[33] Several clean glass substrates were then functionalized with 3-cyanopropyldimethylchlorosilane following the same procedures used to functionalized GNP membranes. Lipids were introduced to the substrates via the vesicle fusion method,[30−32] rather than the painting method outlined above. The reason for using vesicle deposition is, as expected, painting did not yield macroscopically uniform films over the entire glass surface. Thus, vesicle fusion was employed instead to create large uniform regions for microscopy and spectroscopy measurements. It is assumed that the method of applying the lipids to the substrate does not change the way the lipid molecules orient.

A POPC vesicle solution was incubated above a glass surface for 20 min, and then excess solution was rinsed away and replaced by 1.0 M KCl, 10 mM PBS buffer solution (pH 7.4). Following the rinsing step, the surface was gently scratched with a pair of metal tweezers. Following the scratching step, the sample was rinsed again to remove any lipid material that separated from the surface during scratching. The fluorescence images on the left side in Figure 4 are micrographs of lipid

(35) Riehn, R.; Austin, R. H., *Anal. Chem.* **2006**, *78*, 5933−5934.
(36) Wang, G.; Zhang, B.; Wayment, J. R.; Harris, J. M.; White, H. S. *J. Am. Chem. Soc.* **2006**, *128*, 7679−7686.
(37) Adamson, A. W.; Gast, A. P. *Physical Chemistry of Surfaces*, 6th ed.; John Wiley & Sons: New York, 1997.
(38) Mueller, P.; Tien, H. T.; Wescott, W. C.; Rudin, D. O. *Circulation* **1962**, *26*, 1167−1171.
(39) Alverez, O. How to Set Up A Bilayer System. In *Ion Channel Reconstitution*; Miller, C., Ed.; Plenum Publishing Co.: New York, 1986; pp 115−130.
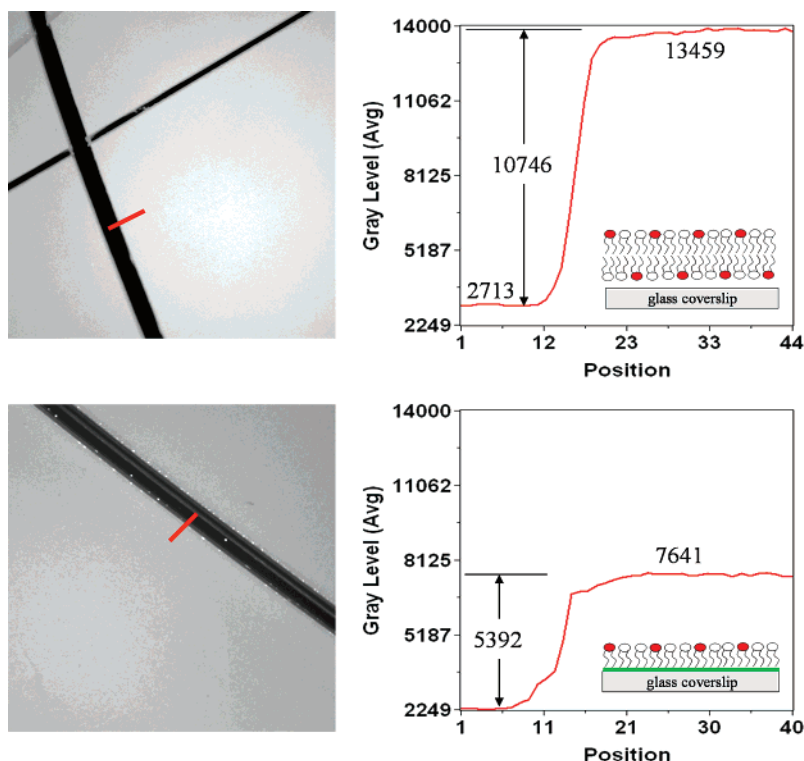
Figure 4. Fluorescence micrographs of a POPC lipid bilayer on bare (unmodified) glass (upper panel) and a lipid monolayer on silanized glass (lower panel). The linescan to the right of each image corresponds to the red lines in each image and shows the relative fluorescence levels of bilayer and monolayer with respect to the background. The scratch marks (black) were intentionally made with a tweezers to determine the background level.

layers on the bare glass (upper image) and on the cyano-terminated glass (lower image). Line scans of fluorescence intensity that correspond to the red lines drawn on the images are presented to the right of the corresponding fluorescence images. Both line scans have similar background levels (corresponding to the dark regions in the scratched area), yet the hydrophilic bare glass substrate displays precisely twice the specific fluorescence as the silanized glass sample. It is well-known that lipid *bilayers* fuse to plain glass substrates.[30−32] Therefore, the 50% decrease in fluorescence obtained from the cyano-terminated glass substrate, relative to the lipid bilayer on bare glass, is consistent with the formation of a lipid *monolayer*.

The fluidity of the putative monolayer structure was examined using the fluorescence recovery after photobleaching (FRAP) technique (Figure 5).[34] Surface-bound fluorescently labeled lipid layers on glass surfaces were bleached momentarily with a laser beam, and the fluorescence recovery of the photobleached spot was measured as a function of time. A single-exponential equation was fit to the data, from which the mobile fraction of the dye-labeled lipids and the half-time of recovery ($t_{1/2}$) were obtained. The diffusion coefficient, D, of lipids in the layers were calculated from eq 1. Figure 5 (top) shows a representative FRAP curve for a bilayer on bare glass, from which the best fit of eq 1 yields a diffusion coefficient value of 3.5 μm^2/s and a recovery of 97%. The curve for the lipid monolayer on silanized glass (bottom) yields a slightly lower diffusion coefficient (0.8 μm^2/s) and a recovery of 91%. The smaller diffusion coefficient of lipids at the silanized glass is consistent with previous results which suggest that frictional interactions between a lipid monolayer and an underlying immobile monolayer lead to slower lipid diffusion.[40] The FRAP results are compelling

evidence for a lipid monolayer structure on the cyano-modified glass surface.

Evidence for the degree of order and orientation of the lipid monolayer were obtained by vibrational sum frequency spectroscopy. VSFS is a surface-specific nonlinear optical technique capable of submonolayer sensitivity at the solid/liquid and liquid/vapor interfaces.[41,42] The relative orientation between a surfactant monolayer and the orientation of interfacial water molecules can be determined by the interference between the −OH and −CH stretch modes in the VSFS spectrum.[43−45] The orientation of the water dipoles depends upon the charge at the interface. For example, a positively charged surfactant situated at an air/water or oil/water interface will lead to water orientation with the oxygen atoms facing toward the interface. Conversely, negatively charged interfaces will cause water to orient with the hydrogen atoms facing toward the interface. In both cases, the alkyl chains of the surfactant face toward the hydrophobic phase.[43−45] When the interface is positively charged this manifests itself as constructive interference around 2980 cm^{-1} (i.e., the region between the −OH and −CH stretch regions) in the VSFS spectrum. Therefore, the lipid monolayer orients with the hydrophobic tail groups facing toward the substrate and the hydrophilic groups facing toward the solutions (Figure 6 inset). On the other hand, destructive interference from a negatively charged surfactant monolayer will cause the VSFS signal

(40) Howland, M. C.; Sapuri-Butti, A. R.; Dixit, S. S.; Dattelbaum, A. M.; Shreve, A. P.; Parikh, A. N. *J. Am. Chem. Soc.* **2005**, *127*, 6752−6765.
(41) Shen, Y. R. *The Principles of Nonlinear Optics*; Wiley: New York, 1984.
(42) Richmond, G. L. *Chem. Res.* **2002**, *102*, 2693−2724.
(43) Kim, G.; Gurau, M.; Kim, J.; Cremer, P. S. *Langmuir* **2002**, *18*, 2807−2811.
(44) Chen, X. Y.; Chen, Z. *Biochem. Biophys. Acta* **2006**, *9*, 1257−1273.
(45) Gragson, D. E.; Richmond, G. L. *J. Phys. Chem. B* **1998**, *102*, 3847−3861.

Bilayers on Bare Glass

D=3.5 ± 0.1 μm²

Recovery$_{t\infty}$ = 97%

Bilayers on Silanized Glass
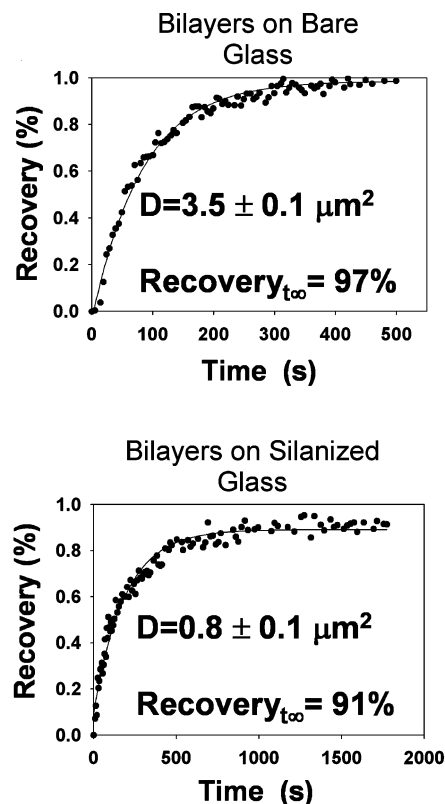

D=0.8 ± 0.1 μm²

Recovery$_{t\infty}$ = 91%

Figure 5. Fluorescence recovery as a function of time of a small photobleached area of a POPC bilayer on bare glass (left) and a POPC monolayer on silanized glass (right). Both lipid structures were doped with 0.1 mol % Texas Red DHPE.
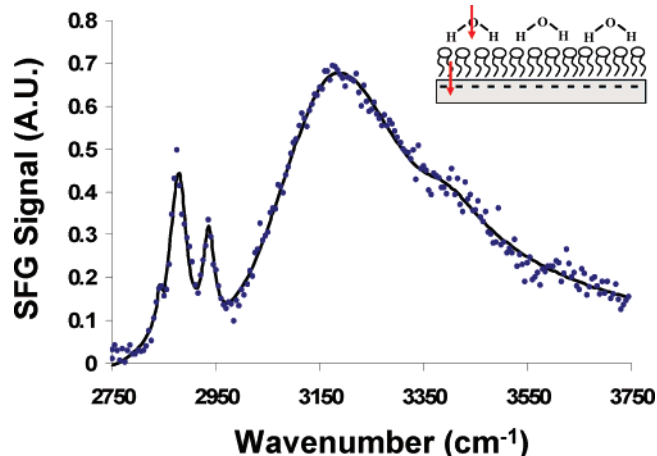

Figure 6. SFG spectrum of a DMPC lipid monolayer on a silanized fused-silica substrate. The region at 2980 cm^{-1} shows a finite signal strength indicating constructive interference between water dipoles and the dipoles of the terminal methyl group on the acyl lipid tails. A schematic representation of the monolayer orientation is shown in the inset.

intensity to drop to near zero at 2980 cm^{-1}. Exploiting this phenomenon allows us to determine the orientation of a lipid monolayer adsorbed to a cyano-silanized glass substrate.

To perform the VSFS experiments, we employed the vesicle fusion method to introduce DMPC lipids to a cyano-silanized fused quartz substrate under aqueous solution. Under these circumstances the interface has a net negative charge because only a fraction of the surface silanols are derivatized with silanes, while some of the remaining silanol groups are typically dissociated at neutral pH.[46] The VSFS spectrum obtained from

this system is shown in Figure 6. Focusing on the region near 2980 cm^{-1}, it is obvious that constructive interference exists between the $-$CH and $-$OH stretch regions. Control experiments of the identical system, but in the absence of the lipid monolayer demonstrated that the $-$CH stretch range signal originated nearly exclusively from the lipid monolayer rather than the cyano-terminated monolayer. Moreover, the overall strength of the $-$CH$_3$ stretch modes observed in Figure 6 is consistent with a relatively well-ordered lipid monolayer.[42−45]

Single Ion-Channel Recordings. Reconstitution of wild-type α-hemolysin (WTαHL) from monomer peptide produced by *Staphylococcus aureus* was investigated in POPC and DPhPC lipid bilayers suspended across GNP membranes with orifice radii between 100 and 400 nm. WTαHL is a well-characterized transmembrane protein comprising seven 293-amino acid, 33.2 kDa, water-soluble, polypeptide monomers that form heptameric pores in lipid bilayers.[47] The channel conductance in 1.0 M KCl has been reported to be in the range of ~1 nS.[48]

We have discovered that a small positive transmembrane pressure, P_T ($>$20 mmHg), is required for insertion of a WTαHL. This phenomenon is described in more detail in a later section in which we demonstrate the capability, using specialized instrumentation, of quantitatively controlling protein insertion and removal by varying P_T. Here, we note that a small positive P_T can be achieved by simply sealing the back end of the GNP capillary (and the Ag/AgCl electrode inserted through the open end) with a 100% silicon rubber sealant. The sealing process compresses the air and solution inside the capillary, inducing a small (and unmeasured) positive P_T. Using sealed GNP capillaries, WTαHL spontaneously and reproducibly inserts into the suspended bilayer and exhibits stable ion-channel behavior in full agreement with literature reports. Insertion of a functioning WTαHL channel does not occur in the absence of the seal, unless other means are employed to create a positive P_T.

The insertion of a WTαHL ion channel into a suspended lipid bilayer, and subsequent stochastic binding of heptakis(6-O-sulfo)-β-cyclodextrin (s$_7\beta$CD) to the channel, is demonstrated in the $i-t$ plot shown in Figure 7A. The data in the figure correspond to a DPhPC lipid bilayer suspended across the orifice of a 250 nm-radius GNP membrane. Prior to bilayer painting, the GNP capillary was filled with a 3 μM WTαHL (monomer form), PBS buffer solution (pH 7.4) and the open end of the GNP capillary was sealed with silicon rubber sealant to create a positive P_T. The GNP capillary was then immersed into a PBS buffer solution (pH 7.4) containing 100 μM s$_7\beta$CD, and the ionic current through the GNP orifice was monitored while applying a constant potential of $-$40 mV. Following bilayer formation (as evidenced by a sudden decrease in current, see Experimental Section), the step increase in ionic current observed in the $i-t$ trace (Figure 7A) at $t = 6$ s corresponds to a conductance of 900 pS, in excellent agreement with the reported conductance of WTαHL in 1.0 M KCl. Analogous experiments demonstrate that WTαHL can also successfully be inserted into the suspended lipid bilayer by addition of a protein monomer to the external solution. On the basis of 20 measurements using different GNP membranes and WTαHL channels, the average conductance was measured to be 890 ± 90 pS.

(46) Iler, R. *Chemistry of Silica*; Wiley: New York, 1979.
(47) Gouaux, E. *J. Struct. Biol.* **1998**, *121*, 110−122.
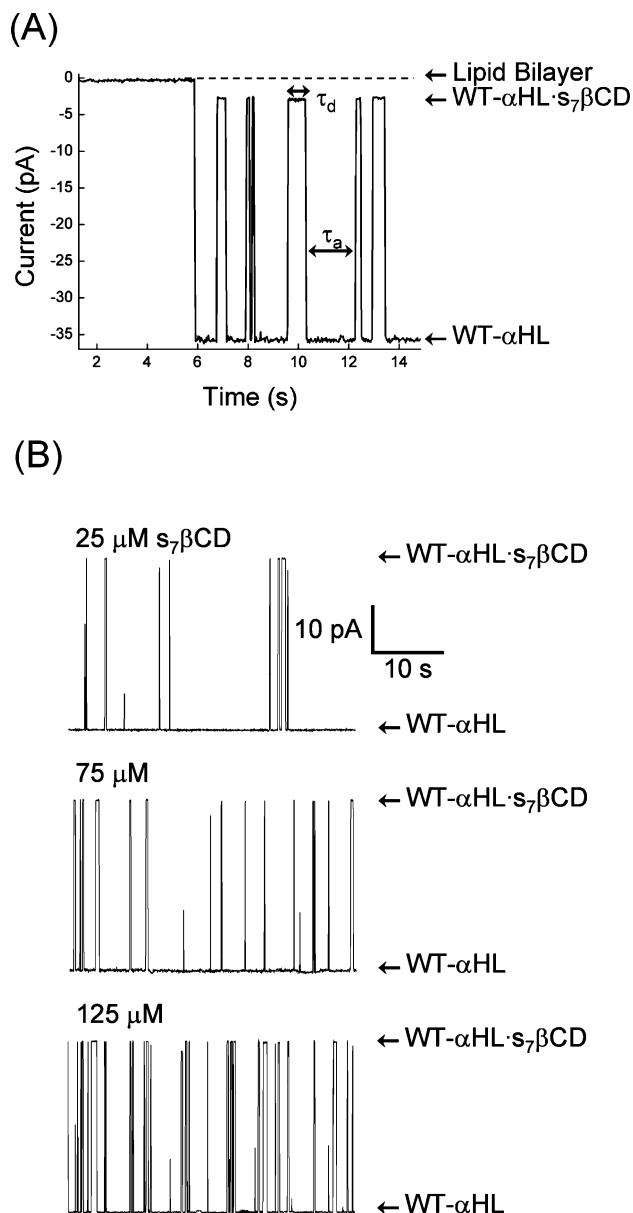(48) Deamer, D. W.; Branton, D. *Acc. Chem. Rev.* **2002**, *35*, 817−825.

(A)

(B)

Figure 7. (A) An $i-t$ trace corresponding to (i) the baseline current associated with a DPhPC bilayer spanning a 250 nm-radius pore (0 to ~6 s); (ii) the insertion of a single WTαHL-channel at ~6 s; and (iii) binding of individial $s_7\beta$CD molecules to the WTαHL channel. Data were recorded at a DC bias of −40 mV in a 1.0 M KCl 10 mM PBS buffer solution at pH 7.4. The single-channel conductance of the αHL channel is measured to be 900 pS. The buffered electrolyte inside the GNP capillary contained 3 μM WTαHL, while the outside buffered electrolyte contained 100 μM [$s_7\beta$CD]. Binding dwell times, τ_d, and the time between binding events, τ_a, are labeled on the figure. (B) $i-t$ traces showing $s_7\beta$CD binding events in solutions containing 25, 75, and 125 μM $s_7\beta$CD, respectively, while applying a potential of −40 mV.

WTαHL has been extensively investigated as a sensing component for the stochastic detection of single molecules.[11] In the experiment described here, $s_7\beta$CD transiently binds, noncovalently, in the lumen of the WTαHL pore from the trans side of the membrane.[49] Reversible binding of $s_7\beta$CD results in a temporary 92% reduction in conductance of the protein.[49] Figure 7A shows resistive pulses, in the time frame between 6 and 14 s, corresponding to single binding events of $s_7\beta$CD to

(49) Gu, L.; Serra, M. D.; Vincent J. B.; Vigh, G.; Cheley, S.; Braha, O.; Bayley, H. *Proc. Natl. Acad. Sci. U.S.A.* **2000**, *97*, 3959−3964.

WTαHL. We find that the WTαHL channel conductance is reduced by 93.1 ± 0.5%, in agreement with literature reports. The frequency of $s_7\beta$CD binding is strongly voltage dependent as previously reported (results not shown),[50] and the expected concentration dependence is seen. Figure 7B shows three representative $i-t$ plots of $s_7\beta$CD detection in a single WTαHL channel over the 250 nm-radius GNP membrane as a function of $s_7\beta$CD concentrations (25, 75, and 125 μM). As expected, time between binding events decreases as the cyclodextrin concentration is increased. These experiments and others demonstrate the existence of a bilayer suspended across the GNP membrane orifice.

Pressure Controlled Insertion and Removal of Trans-membrane Protein. A home-built pressure rig (Figure 2B) was used to control and maintain P_T to quantitatively investigate the influence of P_T on WTαHL insertion rates. The experiment is performed by applying a positive or negative P_T (between −100 and 350 mmHg) inside the capillary relative to the external solution.

Figure 8A shows a $i-t$ plot of the pressure controlled insertion and removal of WTαHL. In this experiment, a DPhPC bilayer is painted across a 190 nm-radius GNP membrane. The internal solution contained 3 μM WTαHL and the PBS buffer solution (pH 7.4), while the external solution contained only the PBS buffer (pH 7.4). To confirm protein insertion and removal, the ionic current was monitored while applying a constant voltage of −40 mV. In the initial stage of the experiment, and as long as $P_T = 0$, no protein channels insert in the bilayer. At $t = 5$ s, P_T is increased to ~100 mmHg, resulting in a single WTαHL insertion at $t = 7$ s. A second WTαHL channel inserts into the bilayer at $t = 9$ s. At $t = 11$ s, the pressure is reduced to −40 mmHg, resulting in the sudden removal of both WTαHL channels. We note that the suspended lipid bilayer membrane remains intact during the variations in P_T and the insertion/removal steps can be repeated indefinitely using the same bilayer. Figure 8A shows the insertion and removal of two additional WTαHL channels in the time period between 15 and 25 s.

Figure 8B shows a plot of the insertion rate of the *first* WTαHL channel into the DPhPC bilayers suspended across the orifices of three different GNP membranes with different radii (120, 190, and 250 nm). In these experiments, each GNP capillary was filled with a PBS buffer solution (pH 7.4) containing 1.5 μM WTαHL prior to formation of a DPhPC bilayer. After insertion of a single WTαHL pore into the bilayer, a negative pressure was used to remove it, and the experiment was repeated. Inspection of Figure 8B demonstrates that the rate of WTαHL insertion increases roughly linear with P_T. The slopes of the lines in Figure 8B also suggest that insertion rates scale roughly in proportional to the radius of the GNP membrane orifice, or equivalently, the area of the lipid bilayer. In addition, the nonzero intercepts for all three lines clearly indicate that a threshold P_T of ~20 mmHg is required for insertion of a WTαHL channel into the GNP membrane/bilayer structure. This latter finding is consistent with the observation discussed above that WTαHL channels do not insert into suspended bilayers on unsealed ($P_T = 0$) GNP membranes.

In additional experiments, WTαHL insertion from the *external* solution into the suspended bilayer was investigated

(50) Gu, L.; Cheley, S.; Bayley, H. *Science* **2001**, *291*, 636−640.
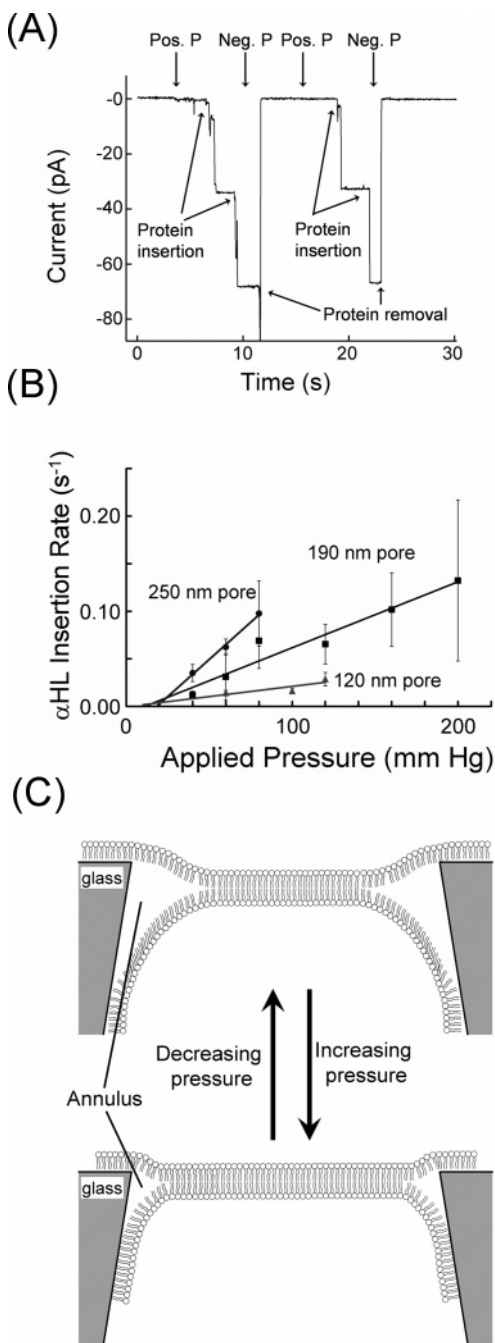
Figure 8. (A) An $i-t$ trace showing the controlled insertion and removal of WTαHL channels as a function of the transmembrane pressure. In this example, a 100 mmHg transmembrane pressure is applied (inside capillary vs outside pressure) at $t = 5$ s, followed by spontaneous insertion of two WTαHL channels at ∼7 and 9 s. The two channels are then removed by applying a −40 mmHg transmembrane pressure at ∼11 s. A second controlled insertion and removal of two additional WTαHL-channels is shown in the time period between 15 and 25 s. (B) Plot of the rate of the first WTαHL insertion as a function of transmembrane pressure for 250, 190, and 120 nm radius GNPs. (C) Schematic drawing of the proposed bilayer and annulus region of the lipid bilayer over the pore orifice as a function of the applied pressure.

as a function of P_T (data not shown). Using the same sign convention for P_T (internal solution vs external solution), the results are qualitatively similar as described above for insertion of WTαHL from the *internal* solution. This finding indicates the dependence of insertion rates on P_T is not a consequence of pressure-induced flow, but rather reflects a change in the curvature or surface area of the bilayer as P_T is varied.

The mechanism by which P_T influences the insertion and removal of WTαHL is not yet fully understood. We speculate that variations in P_T result in an increase or decrease in bilayer area or lead to changes in the curvature of the bilayer that alter the kinetics and energetics associated with transferring the protein from the solution to the bilayer (and vice versa), or between the lipid bilayer and the lipid monolayer. It has been previously demonstrated that hydrostatic pressure influences the cross-sectional area of a lipid bilayer film suspended across larger orifices.[51] The pressure induced changes in lipid bilayer area are associated with the equilibrium between lipids in the bilayer and the lipid/hydrocarbon annulus region between the bilayer and support orifice, as depicted in Figure 8C for GNP suspended bilayers. Quantitatively, the effect of hydrostatic pressure differences is given by the law of Laplace:[51]

$$\Delta P = 2\gamma/R \qquad (2)$$

where γ is the interfacial tension (mN/m), R is the radius of curvature (m), and ΔP is the hydrostatic pressure difference (mN/m^2) across the bilayer. In the case of planar lipid bilayers, R is used to describe the portion of the lipid film between the support orifice and the border of the annulus and bilayer.[51] As P (or P_T) increases, R decreases resulting in an increase in the exposed bilayer area. The resulting increase in bilayer area is expected to result in greater probability of a WTαHL insertion, regardless of which side of the bilayer that is presented to the protein for insertion. Albeit speculative at the current time, the observed increase in insertion rate with increasing P_T is consistent with this picture. The asymmetric geometry of the conical-shaped nanopore is clearly associated with the asymmetry in the pressure dependence, that is, a negative P_T results in removal of the protein and a positive P_T induces protein insertion.

The bilayers suspended across the GNP orifices are susceptible to pressure induced rupture. The rupture pressure (∼80 mmHg to greater than 300 mmHg) varies significantly with pore size and the mole fraction of lipid/decane solution employed to paint the bilayers. Studies are currently underway to quantify these relationships and will be reported in the future.

GNP Membrane/Lipid Bilayer Stability Measurements and Lifetime. Preliminary estimates of the stability of POPC and DPhPC bilayers suspended over GNP membranes were obtained by measuring the breakdown voltage, the susceptibility of failure from mechanical disruptions, and the lifetime of bilayers with and without WTαHL channels. As an initial qualitative measure of stability, we note that suspended bilayers on the GNP membrane containing a functioning WTαHL channel can be manually transported between different solutions while maintaining electrical conductivity with a water droplet at the end of the glass capillary.

The electrical voltage stability of the suspended bilayer (without ion channel) was examined in PBS buffer solutions (pH 7.4). Bilayers were formed using the painting method (as described above) and then the potential was scanned at 50 mV/s while monitoring current. Using three GNP membranes (150, 150, and 100 nm-radius), an average breakdown voltage of 770 ± 150 mV was recorded, greatly exceeding the recently reported

(51) White, S. H. The Physical Nature of Planar Bilayer Membranes. In *Ion Channel Reconstitution*; Miller, C., Ed.; Plenum Publishing Co.: New York, 1986; pp 115−130.

values of 325 [20] and 460 mV.[1] Along with improved voltage stability, bilayers suspended on the GNP membrane are able to withstand rigorous stirring of solution without breakage.

Bilayer lifetimes were measured in a sealed glass cell to avoid solvent evaporation. Bilayers were painted over several GNP membranes, and the seal resistance was monitored as a function of time using an alternating current signal between two Pt electrodes. Lifetimes of ∼2 weeks were routinely achieved. Bilayers with WTαHL channels inserted from the inside of the capillary were also tested for lifetime stability using Ag/AgCl electrodes as described in the Experimental Section. Once protein was inserted, $s_7\beta CD$ was added to confirm a functioning protein channel existed in the bilayer. Lifetimes of these experiments were typically on the order of 24 h with continuous stochastic detection, but it should be noted that the primary reason for failure was a loss of transmembrane pressure (due to leaks in in-lab-built system) causing the WTαHL to spontaneously come out of the bilayer. Recently, with an improved pressure system, several continuous measurements of $s_7\beta CD$ detection have recently lasted >200 h and one measurement for over 400 h. Thus, although optimization of device lifetime has not yet been vigorously pursued, ion-channel recordings are routinely accomplished using the GNP platform throughout a full day, with preliminary evidence that the inherent lifetime may be much greater (e.g., weeks or months).

Conclusion

The GNP membrane is a very promising new support structure for ion-channel recordings. We have demonstrated that a nanopore in glass can be chemically modified to impart intermediate hydrophobic surface character that allows simultaneous formation of a suspended lipid bilayer and the wetting of the nanopore. GNP membranes with orifice radii as small as 100 nm have successfully been used for ion-channel recordings, reducing by 10^6-fold the exposed area of the lipid bilayer in comparison to conventional measurements. Greatly enhanced mechanical and voltage stabilities result from the reduction in bilayer area, yielding a robust ion-channel recording system in aqueous solutions without the need to encapsulate the bilayer in viscous gels and polymers.

We have demonstrated that reconstitution of the heptameric transmembrane protein, WTαHL, readily occurs in lipid bilayers suspended over GNP orifices that have radii as small as 100 nm. Furthermore, the resulting ion-channel functions identically to WTαHL in conventional measurements using large-area orifices in Teflon and other polymeric membranes (i.e., same

conductance and single-molecule binding rates). Thus, although the radius of the orifice in glass is only ∼10× larger than that of the size of the protein ion channel, the similarity of these dimensions does not appear to impart any adverse or anomalous behavior. We are currently investigating lipid bilayer formation and insertion of WTαHL using GNP membranes with orifice radii significantly smaller than those reported here.

We have additionally demonstrated that the transmembrane pressure can be used to *reproducibly* control the insertion and removal of WTαHL from lipid bilayers that are suspended across the GNP orifice. This remarkable new capability may prove to be an important processing component for spatially directed insertion of proteins at different orifices of array-based ion-channel biosensors. From a fundamental view, this phenomenon will require new experiments and theory to understand how pressure influences the suspended bilayer structure, as well the mechanisms underlying protein insertion and removal as pressure forces are exerted on the bilayer.

Although not exploited in the present body of work, the small size of the GNP orifice also presents advantages in improved signal processing. In particular, because the lipid bilayer capacitance is considered a major contributor to overall system noise, the GNP membranes, with 10^6-fold reduction in bilayer area, are likely to be candidates in low-noise ion-channel applications.[17] We are currently pursing applications of the GNP membrane for ion-channel recordings using alternating current methods.[52]

Finally, we note that the GNP membranes employed here, and described in detail elsewhere, are fabricated by routine benchtop methods using materials and instruments commonly found in most chemical laboratories and, specifically, do not require microlithographic fabrication techniques.[24] Thus, the GNP membranes are assessable for ion-channel recordings to a wide community.

(52) Ervin, E. N.; White, R. J.; Owens, T. O.; Tang, J. M.; White, H. S. *J. Phys. Chem. B* **2007**, *111*, 9165−9171.